Vol 18 No 4, April 2009
1674-1056/2009/18(04)/1469-04

Chinese Physics B

© 2009 Chin. Phys. Soc.
and IOP Publishing Ltd

Tunable phase-stabilized infrared parametric laser source*

Zhang Chun-Mei(张春梅)[a], Wang Jian-Liang(王建良)[a], Wei Peng-Fei(尉鹏飞)[a], Song Li-Wei(宋立伟)[a], Li Chuang(李 闯)[a], Kim Cheol-Jung(金哲中)[b], and Leng Yu-Xin(冷雨欣)[a]†

[a] *State Key Laboratory of High Field Laser Physics, Shanghai Institute of Optics and Fine Mechanics, the Chinese Academy of Sciences, Shanghai* 201800, *China*
[b] *Korea Atomic Energy Research Institute, Yusung, Taejon* 305-353, *Korea*

(Received 3 July 2008; revised manuscript received 5 August 2008)

This paper reports that the tunable self-phase-stabilized infrared laser pulses have been generated from a two-stage optical parametric amplifier. With an 800 nm pump source, the output idler pulses are tunable from 1.3 μm to 2.3 μm, and the maximum output energy of the idler pulses is higher than 1 mJ at 1.6 μm by using 6 mJ pump laser. A carrier-envelope phase fluctuation of ∼0.15 rad (rms) for the idler pulses is measured for longer than one hour by using a home build f-to-2f interferometer.

Keywords: phase-stabilized, infrared parametric laser, optical parametric amplifier, tunable
PACC: 3320E, 4265K, 7830G

1. Introduction

To obtain attosecond pulses from high harmonic generation (HHG), an ultra-fast intense driving laser pulse with carrier-envelope phase (CEP) stability is desirable.[1−4] According to previous works, the CEP of driving pulses is a critical parameter in HHG for isolated attosecond pulses generation and measurement.[5,6] Further, to obtain wider and higher energy harmonic supercontinuum for shorter attosecond pulses, the cut-off energy of HHG should be increased, and therefore longer driving laser wavelength is highly desirable. But the quantum-mechanical diffusion of the electron wave packet due to the longer transit time in the continuum leads to reduce HHG efficiency for longer carrier wavelength. Then the driving laser with 1.5 μm to 3 μm central wavelength is regarded as the balance for these two conflicting requirements.[7]

The CEP stabilized pulses have been obtained from Ti:sapphire laser directly with active CEP control technique, and 50 mrad (rms) CEP stabilization has been demonstrated,[8] but the laser wavelength is near 800 nm limited by the Ti:sapphire crystal. In order to obtain the CEP stabilized pulses in 1.5–2 μm region, the difference-frequency generation (DFG) has been exploited.[9−10] Comparing with the active CEP stabilization, the CEP of pulses is stabilized passively and easily with DFG process. There are two methods for CEP stabilized pulses generation with DFG. One is that the CEP stabilized seed is generated by DFG process within a single pulse, the seed is amplified in following optical parametric amplifier (OPA) stages. The 1.5 μm pulses with the energy up to 1.2 mJ and pulse duration down to 17 fs, characterized by 0.25 rad (rms) CEP fluctuation have been obtained.[9] Another is that the CEP stabilized idler pulses are generated in OPA process directly, if the pump and signal pulses are from the same laser source with same carrier phase offset. Near 2 μm pulses with 0.33 mJ energy and 55 fs duration, characterized by < 0.1 rad (rms) CEP fluctuation have been generated.[10] The latter method is more stable and simpler in implementation without using a DFG stage for seed generation.

2. Experimental setup

In this work, we demonstrate a Ti:sapphire pumped OPA, the CEP fluctuation of the idler pulses from the OPA is ∼0.15 rad (rms) for longer than one

*Project supported from the National Basic Research Programme of China (Grant No 2006CB806001), the Knowledge Innovation Program of the Chinese Academy of Sciences (Grant No KGCX-YW-417), and Shanghai Commission of Science and Technology (Grant Nos 07JC14055, 06DE22015 and 0652nm005), and Japan-Korea-China Cooperative Project on "High Energy Density Sciences for Laser Fusion Energy".
†Corresponding author. E-mail: lengyuxin@siom.ac.cn

hour. The maximum parametric conversion efficiency in the final OPA stage is ∼40% with 1 kHz high energy pump energy, and the tunable range of the OPA output is 1.3 μm–2.3 μm for signal pulses, 2.3 μm–1.3 μm for idler pulses. With 6 mJ/1 kHz total pump energy, $>$ 1 mJ idler pulses at 1.6 μm with 1 kHz repetition rate have been demonstrated.

Figure 1 shows the experimental setup. The driving pulses are from a commercial Ti:sapphire laser (Coherent LEGEND-HE-Cryo), providing 10 mJ pulses at 800 nm with 1 kHz repetition rate. In this experiment, driving energy up to only 6 mJ has been used for $>$ 1 mJ idler pulses generation, and as we know this is the highest pump energy and output idler energy used in OPA system at kHz repetition rate. The OPA setup is similar to our previous work.[11] A fraction of laser beam (90 μJ) was split and focused into a 2 mm-thick sapphire plate to generate a single-filament white light continuum (WLC) with an excellent radial intensity profile, giving rise to spectral broadening. The other fraction of laser beam (110 μJ) is used to pump the first noncollinear OPA stage (NOPA1) consisting of a 2 mm-thick BBO plate (cut for type I phase match) and seeded by the WLC. The WLC pulse was amplified up to 10 μJ of energy in NOPA1. In NOPA1, the power density of the pump pulses on the crystal is optimized to obtain the best spatial beam quality for the output pulses. In NOPA2, to match the beam size of the seed and the pump pulses on the crystal, we expand and collimate the seed beam with a Kepler 1:4 telescopes. The output of NOPA1 seeded a high-energy amplification stage (NOPA2) using a 3 mm-thick BBO plate (cut for type II phase match).

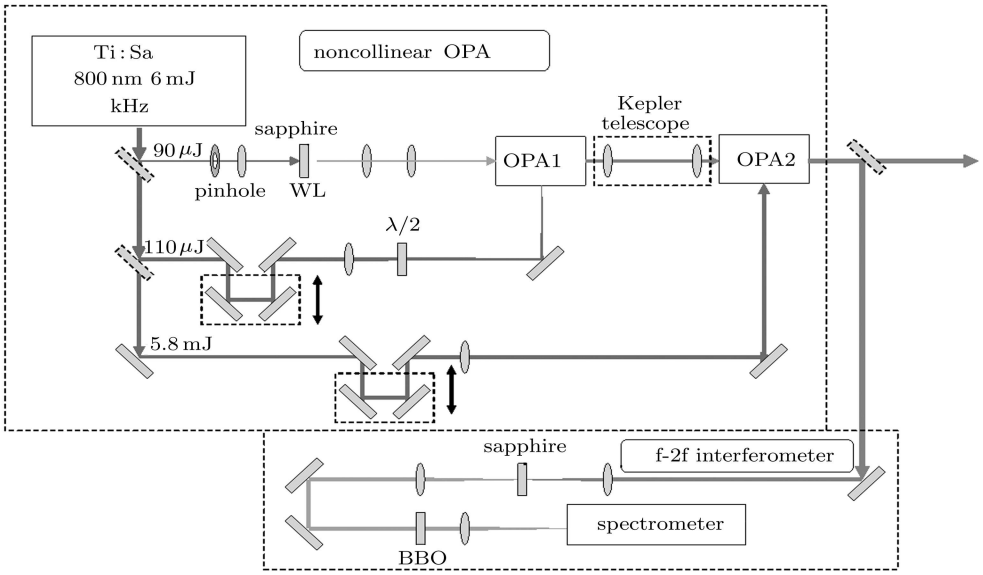


Fig.1. Experimental setup for the generation of high-energy self-phase-stabilized pulses and f-2f interferometer: Ti:Sa, CPA Ti:sapphire laser.

After being amplified in NOPA2, we can obtain the idler pulses with central wavelength tunable from 1.3 μm to 2.3 μm, as shown in Fig.2(a). At the same time, we can get the signal pulses with central wavelength tunable from 1.3 μm to 2.3 μm respectively, as shown in Fig.2(b).

In both the two OPA stages, the pump intensity is nearly 100 GW/cm^2 by controlling the pump beam size inside the BBO crystals, just below the threshold of filament or other nonlinear process generation in the crystal. The bandwidth and central wavelength of the signal or idler pulses can be tuned and optimized by adjusting the crystal phase-matching angle and the pump pulses. The pump conversion efficiency of the NOPA2 stages is up to about 40%, as shown in Fig.3. The maximum total OPA conversion efficiency is 40% with idler pulse near 1.6 μm for near degenerate noncollinear OPA. At the degenerate wavelength, with the pump energy of NOPA2 about 5.8 mJ, NOPA2 can produce idler pulse with energy of 1.19 mJ, and signal pulse with energy of 1.12 mJ with optimization.

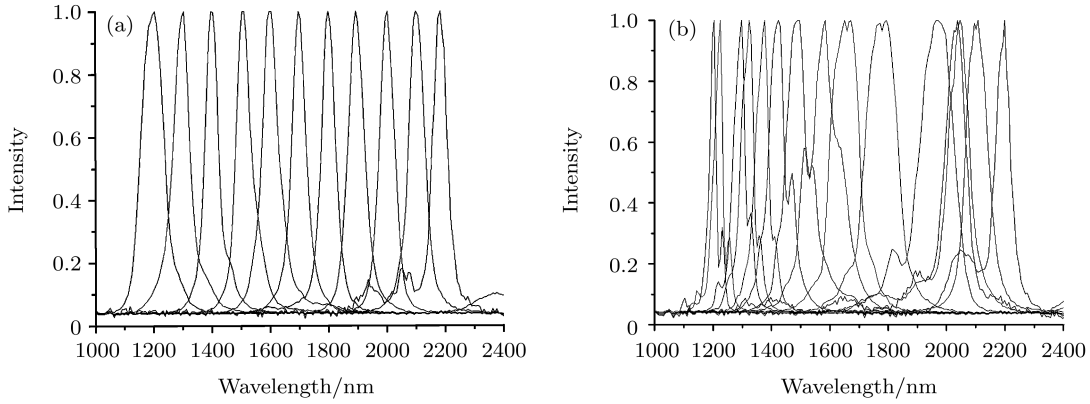


Fig.2. Normalized spectra of the OPA2 output pulses. (a) The idler pulses spectra with tunable central wavelength from 1.3 μm to 2.3 μm, (b) The signal pulses spectra with tunable central wavelength from 1.3 μm to 2 μm.

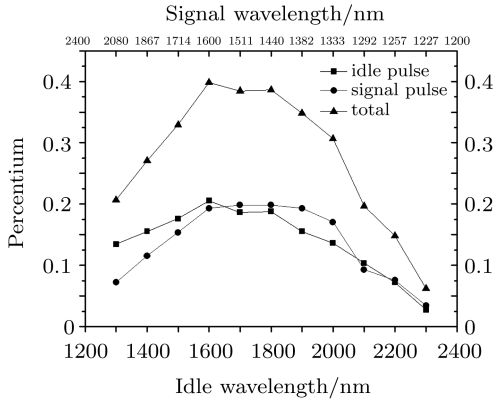


Fig.3. OPA conversion efficiency curve in the final OPA stage with 5.8 mJ pump pulses, the highest total conversion efficiency up to $\sim$ about 40% is at 1.6 μm wavelength.

3. Pulse characterization

The signal, idler and pump pulses durations are measured by a single-shot second-order autocorrelator. When the measured pump pulse duration is 35 fs by the autocorrelator, the idler pulse duration is about 36 fs at 1.6 μm, and the signal pulse duration is about 37 fs also at 1.6 μm without any compression.

A number of CEP measurement methods[12−15] have been proposed and demonstrated. Here, we characterized the infrared (IR) pulses CEP stability with a homemade f-to-2f interferometer. A fraction of the idler pulse energy is first focused onto a 2 mm-thick sapphire plate, to generate WLC, and then the residual idler light is frequency doubled in a 100 μm-thick BBO crystal. The fundamental frequency (FF) and second harmonic (SH) pulses spatially overlapped are directed to a polarizer to project the same polarization. For 1.8 μm incident pulses, the frequency overlap between the FF and the SH is achieved in the 1100–1200 nm wavelength range and measured with a spectrometer. The temporal evolution of the phase-dependent interference pattern is shown in the lower panel of Fig.4. The measured CEP fluctuation is sensitive to the environmental noise strongly. The upper panel of Fig.4 reports the phase fluctuations over longer than one hour measurement, giving a CEP fluctuation with 0.1433 rad (rms). Further, the CEP stabilization of the other tunable wavelengths is demonstrated. Such fluctuations are attributed mainly to the instability of the OPA and f-2f systems for the environmental noise, and the energy fluctuation in the sapphire plate still introduces the phase fluctuations. This measurement is a clear proof of the shot-to-shot stability of the CEP.

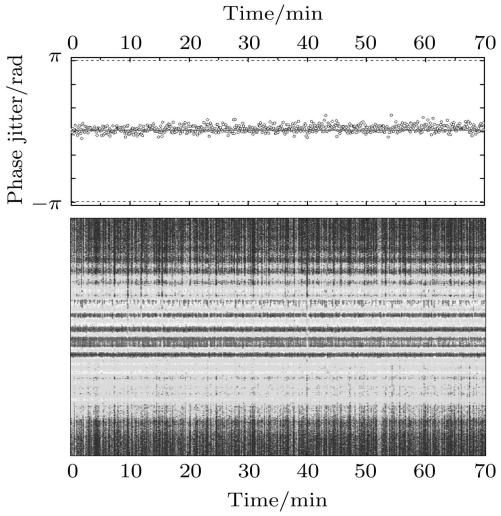


Fig.4. Lower panel, temporal evolution of the phase-dependent interference pattern acquired over one hour. Upper panel, the measured CEP fluctuations of 0.1433 rad (rms) for 1.8 μm incident pulses.

4. Conclusions

In summary, we have developed a femtosecond noncollinear OPA with broadband tunable range in IR region, which consists of a WLC and two noncollinear OPA stages. The CEP fluctuation of the idler pulses from the OPA is ∼0.15 rad (rms) in longer than one hour. The total tunable range for signal and idler pulses is from 1.3 μm to 2.3 μm, and the maximum conversion efficiency in the final OPA stage reaches about 40%. Under near degenerate noncollinear OPA condition, we have demonstrated 1.19 mJ idler pulses near 1.6 μm and 1.12 mJ signal pulses near 1.6 μm, corresponding to the maximum 40% conversion efficiency under 5.8 mJ pump condition in the second OPA stage. This high-energy ultrafast CEP stabilized source is useful in many applications, such as attosecond pulses generation.

References

[1] Baltŭska A, Udem T, Uiberacker M, Hentschel M, Goulielmakis E, Gohle C, Holzwarth R, Yakovlev V S, Scrinzi A, Hänsch T W and Krausz F 2003 *Nature* **421** 611

[2] Xiong H, Li R X, Zeng Z N, Zheng Y H, Peng Y, Yang X, Chen X W, Zeng H P and Xu Z Z 2007 *Phys. Rev.* A **75** 051802(R)

[3] Zheng Y H, Zeng Z N, Li X F, Chen X W, Liu P, Xiong H, Lu H, Zhao S T, Wei P F, Zhang L, Wang Z G, Liu J, Cheng Y, Li R X and Xu Z Z 2008 *Opt. Lett.* **33** 3

[4] Zeng Z N, Li R X, Xie X H and Xu Z Z 2004 *Acta Phys. Sin.* **53** 7 (in Chinese)

[5] Sansone G, Benedetti E, Calegari F, Vozzi C, Avaldi L, Flammini R, Poletto L, Villoresi P, Altucci C, Velotta R, Stagira S, De Silvestri S and Nisoli M 2006 *Science* **314** 443

[6] Peng L Y and Starace Anthony F 2007 *Phys. Rev.* A **76** 043401

[7] Vozzi C, Cirmi G, Manzoni C, Benedetti E, Calegari F, Sansone G, Stagira S, Svelto O, De Silvestri S, Nisoli M and Cerullo G 2006 *Optics Express* **14** 10109

[8] Du Q, Zhu J F, Teng H, Yun C X and Wei Z Y 2008 *Chin. Sci. Bull.* **53** 1

[9] Vozzi C, Calegari F, Benedetti E, Gasilov S, Sansone G, Cerullo G, Nisoli M, De Silvestri S and Stagira S 2007 *Opt. Lett.* **32** 20

[10] Hauri C P, Lopez-MartensC R B, Blaga I, Schultz K D, Cryan J, Chirla R, Colosimo P, Doumy G, March A M, Roedig C, Sistrunk E, Tate J, Wheeler J and DiMauro L F 2007 *Opt. Lett.* **32** 7

[11] Wei P F, Li C, Zhang C M, Wang J L, Leng Y X and Li R X 2008 *Chin. Phys. Lett.* **25** 7

[12] Kakehata M, Takada H, Kobayashi Y, Torizuka K, Fujihira Y, Homma T and Takahashi H 2001 *Opt. Lett.* **26** 1436

[13] Kakehata1 M, Fujihira Y, Takada H, Kobayashi Y, Torizuka K, Homma T and Takahashi H 2002 *Appl. Phys.* B **74** S43

[14] Du Q, Han H N, Hou X, Teng H, Wang X L, Wei Z Y and Zhu J F 2008 *Acta Phys. Sin.* **57** 7753 (in Chinese)

[15] Yang W F, Song X H, Gong S Q, Cheng Y and Xu Z Z 2007 *Phys. Rev. Lett.* **99** 133602